Materials Transactions, Vol. 47, No. 8 (2006) pp. 2049 to 2055

Explosive Welding of Titanium/Stainless Steel by Controlling Energetic Conditions

Palavesamuthu Manikandan[1,*], Kazuyuki Hokamoto[2], Andrei A. Deribas[3], Krishnamurthy Raghukandan[4] and Ryuichi Tomoshige[5]

[1]*Graduate School of Science and Technology, Kumamoto University, Kumamoto 860-8555, Japan*
[2]*Shock Wave and Condensed Matter Research Center, Kumamoto University, Kumamoto 860-8555, Japan*
[3]*Lavrentyev Institute of Hydrodynamics SB RAS, 630090 Novosibirsk, Russia*
[4]*Department of Manufacturing Engineering, Annamalai University, Annamalainagar, Cuddalore District, Tamilnadu-608002, India*
[5]*Department of Applied Chemistry, Sojo University, Kumamoto 860-0082, Japan*

Commercially pure titanium and 304 stainless steel were welded using explosive welding technique. The joints were evaluated using optical microscope, scanning electron microscope, energy dispersive spectroscopy and X-ray diffraction. The study indicates the formation of characteristic interfacial oscillations with vortices at high energetic conditions. The reacted products of the vortices have been identified as FeTi and Fe_2Ti intermetallics by X-ray diffraction. Increase in the kinetic energy spent at the interface cause the volume of vortices to increase. Smooth wavy and flat topography has been obtained for thin flyer plates due to less kinetic energy loss. The results demonstrate a good welding interface for multi-layered welding using a thin stainless steel interlayer, as the kinetic energy dissipation at the interface was less.
[doi:10.2320/matertrans.47.2049]

(Received February 6, 2006; Accepted June 5, 2006; Published August 15, 2006)

Keywords: *explosive welding, titanium, stainless steel, characterization, intermetallics, kinetic energy loss*

1. Introduction

Pressure vessels used for the manufacture of purified terephthalic acid, and autoclaves used in pressure acid leaching of metal ores operate at high temperatures, pressures and corrosive conditions. For the manufacture of these vessels titanium is always the center of attraction due to its intrinsic characteristics such as excellent corrosion resistance, high strength to weight ratio and high melting point. Titanium clad steel construction offers a significant cost reduction for such vessels in comparison to solid titanium. Unalloyed titanium JIS TP270 (ASTM Grade1) is the most commonly used material for clad pressure vessel applications. The demanding requirements are driving manufacturing companies to increase their plant capacities and the rigorous corrosion conditions have resulted in most designs to higher strength clads. Unalloyed titanium JIS TP340 (ASTM Grade2) can offer distinct technological advantages over TP270. Based on a favorable combination of factors, including resistance to corrosion, strength and economy, the prime candidate for clad is type 304 stainless steel. The adoption of this combination is based on both technical and economical reasons, as they offer satisfactory service performance as well as considerable savings.[1–3)]

In spite of their numerous effective combination of properties, titanium/304 stainless steel clads are not much in use because of the difficulty in fabrication. It is apparent that the ability to clad these materials is the key to making them more attractive in industrial environments. The unique features of explosive welding technology provide a means to weld metallurgically incompatible metals-titanium and steel. Explosive welding is a solid-state metal joining process that uses explosive force to create a metallurgical bond between two metal components. Although the detonation of explosive generates considerable heat, there is no time for heat transfer to the component metals; thus there is no appreciable change in the microstructure and mechanical properties of the components.[4–11)]

The result of literature search indicates that very limited attempt has been made to study microstructure of Ti/stainless steel clad produced by explosive welding technique.[12,13)] When explosive cladding titanium to steel, it is known that good bonding is achieved when titanium exhibiting low strength and high ductility, TP270 (ASTM Grade1), is clad to steel. Although higher strength alloys such as JIS TP340 (ASTM Grade2) can be bonded directly to steel, the maximum sizes that can be manufactured reliably are too small for cost effective manufacture of autoclaves. Further, the strength of the base metal influences the bonding parameters. Even though stainless steel has low yield strength, it has a high work hardening rate resulting in a significantly greater yield strength at the point of bond creation.[14)] Consequently, the control of bonding parameters becomes more critical for the successful welding of titanium/stainless steel. In order to develop welds that can better withstand the harsh operating conditions in chemical vessels it is necessary to understand the micro structural features at the bonding interface. In this study, due attention has been given to systematically examine the variations in microstructure with the change of experimental parameters. An attempt was made to clad titanium/stainless steel using explosives and the results are reported.

2. Experimental Procedure

The parallel plate configuration of explosive welding was

*Graduate Student, Kumamoto University

Table 1 Experimental conditions.

Test No.	Flyer plate thickness, t_f/mm	Base plate thickness, t_b/mm	Stand off distance, s/mm	Loading ratio, r	Flyer plate velocity, V_p/m·s^{-1}	Dynamic bend angle, β	Horizontal collision point velocity, V_c/m·s^{-1}	Kinetic energy loss, ΔKE/MJ·m^{-2}
E1	5	9	10	0.93	470	10.9°	2450	2.36
E2	5	9	10	1.16	510	11.7°	2500	2.78
E3	5	9	15	1.16	540	12.5°	2500	3.11
E4	5	9	15	1.4	590	13.0°	2600	3.72
E5	3	9	10	1.16	610	15.0°	2350	2.44
E6	3	9	5	1.94	620	14.4°	2500	2.52
E7	3	9	10	1.94	730	16.7°	2500	3.50
E8	3	9	15	1.94	770	17.7°	2500	3.89
E9	3	9	15	2.33	820	18.2°	2600	4.41
E10	1	9	5	2.33	1020	27.5°	2150	2.33
E11	1	9	10	1.75	965	28.6°	1950	2.08

used as detailed elsewhere.[15] Commercially pure titanium (JIS TP340) was used as flyer plate and 304 stainless steel (JIS SUS304) was used as base plate. Plates of 200 mm in length and 90 mm in breadth were used for cladding. The thickness of base plate, t_b, was 9 mm, whereas the thickness of flyer plate, t_f, was varied as 1, 3 and 5 mm. A powder type explosive, PAVEX, of detonation velocity 2000–3000 m·s^{-1} and density 530 kg·m^{-3}, supplied by Asahi Kasei Chemicals Corp., Japan was employed for the experiments. The thickness of the explosive, t_e, and the stand off distance, s, was varied from 15 to 60 mm and 5 to 15 mm, respectively.

Longitudinal cross-sections of all welds along the detonation direction were prepared by standard metallographic procedures. Metallurgical analysis of the samples was conducted using an optical microscope. Further analysis was undertaken using scanning electron microscope (SEM) equipped with energy dispersive spectroscopy (EDS) system. The interfacial reaction products were identified by X-ray diffraction analyses using a diffractometer. Micro-hardness measurements were made using an Akashi HM-103 digital microhardness tester.

3. Results and Discussion

3.1 Microstructural characterization

In the explosive joining process, as the explosive is initiated, the detonation wave accelerates the flyer plate to give the required oblique high velocity collision of the two plates. The flyer plate collides at a velocity V_p onto the parent plate with a collision angle, β. The relationship between the plate velocity and the collision angle is expressed by the following equation:[4]

$$V_P = 2V_D \sin\frac{\beta}{2} \tag{1}$$

where V_D is the detonation velocity of the explosive.

The collision angle β was calculated using the following equation:[16]

$$\beta = \left(\sqrt{\frac{k+1}{k-1}} - 1\right) \cdot \frac{\pi}{2} \cdot \frac{r}{r + 2.71 + 0.184 t_e/s} \tag{2}$$

where r is the loading ratio (mass of explosive for unit mass of flyer plate), t_e and s are explosive thickness and stand off distance respectively. The value of 'k' in eq. (2) is 1.81, 1.96, 2.20, 2.37 and 2.48 for explosive thickness 15, 21, 28, 38 and 48 mm respectively.[15–17] The experimental conditions are shown in Table 1. On collision the kinetic energy of the flyer plate is dissipated to produce very high pressure in the region, so that the strength of the materials is negligible and as a consequence the metal surfaces in the impact region flows hydrodynamically and promote solid state bonding. The amount of kinetic energy lost by the collision is expressed by the following expression:[17]

$$\Delta KE = \frac{m_D m_C V_p^2}{2(m_D + m_C)} \tag{3}$$

where m_D is the mass of the flyer plate per unit area and m_C is the mass of the collided plate per unit area.

The micrograph of titanium-stainless steel explosive weld reveals the characteristic wave transition with vortices that contain intermetallic layer of the participant metals. During explosive welding, a high velocity forward jet is formed between the metal plates, which sweeps away the surface layers on the metals, if the flyer velocity V_p and the collision angle β are in the range for welding. The collision pressure associated with the kinetic energy of the flyer plate causes shear deformation across the surfaces of the plates. The shear deformation together with the momentum of the flyer plate forms a hump ahead of the collision point. Bahrani *et al.*[18] stated that this hump deflects the jet upwards and completely blocks off the jet. The trapped jet forms a vortex, in which the kinetic energy of the jet is dissipated. The heat generated from the jet is not able to rapidly dissipate from the vortex and hence, becomes localized and increases the temperature of the vortex. Cowan *et al.*[19] reported that the trapping of the jet, in particular, occurs in the case of two initially parallel plates, which is extensively used for large plate cladding. Bergman *et al.*[20] based on his experiments on parallel set up, observed that the jet is in the form of a spray of metal particles and the temperature of the jet was higher in air due to the adiabatic compression of gas between the flyer and parent plate and the frictional heating. The dispersed jet containing the two component metals is vigorously circulated

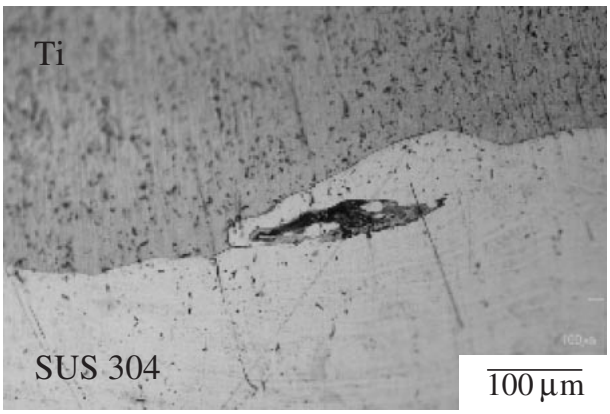

Fig. 1 Optical micrograph of the vortex at low energetic conditions (E5).

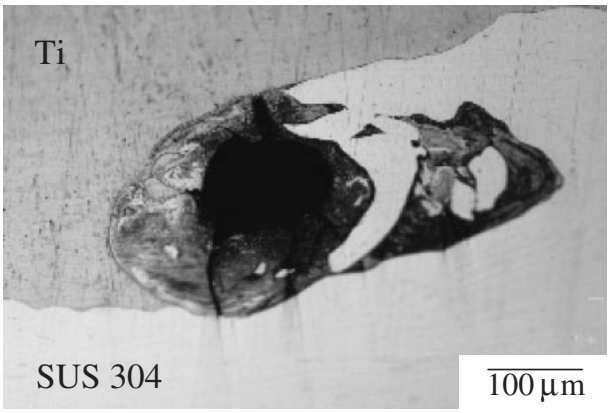

Fig. 2 Optical micrograph of the vortex showing molten zone at high energetic conditions (E9).

in the vortex. The synergistic influence of intermixing of particles and thermal effect would induce the onset of phase transformation.

The nature of the intermetallic formation, which is inherently related to the dissipated energy, was observed to vary for low and high energetic conditions. Consequent to the less dissipation of heat, the reaction between titanium and iron is less and hence, the volume of vortices, hardness and micro cracking is comparatively less in the case of low energy conditions (Fig. 1). At high kinetic energy conditions, dissipated heat causes melting of the mixture, leading to molten zones as shown in Fig. 2. Material reactivity is greatly enhanced by the high energetic conditions leaving more reacted products of the mixture. The binary phase diagram of Ti-Fe shows a decrease in the melting point by the increase in the alloying element, and this provides grounds to assume that much reactivity takes place in the vortex.[21] It was established that the local temperature rise would exceed the melting point of the component metals. Klein[22] deduced that the interface temperature was in the region of 1300–1500°C. Williams *et al.*[23] made a theoretical estimation of the cooling rate in the molten zones and they concluded that they are in the order of 10^5–10^7 K/s. This rapid quenching of the vortex by the surrounding material gives rise to a melt pocket.

Figure 3 represents SEM image and EDS mapping of iron and titanium elements across the vortex. The other alloying

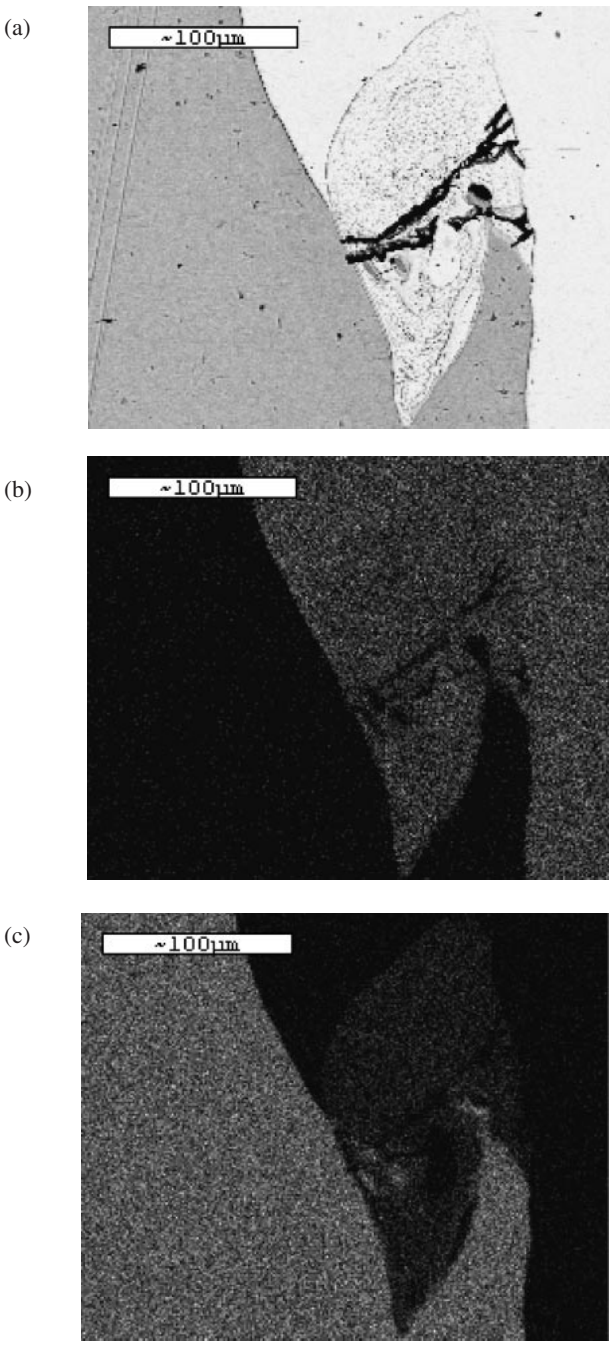

Fig. 3 (a) Representative SEM image and elemental mapping (b) distribution of Fe (c) distribution of Ti (E3).

elements of stainless steel are not shown due to the less percentage of distribution. In general, the recorded images indicate a fairly homogeneous distribution of iron and titanium elements. This is due to the combined effect of vigorous mixing of the jetting material inside the vortex and the high cooling rate. However, in some areas of the vortex titanium was not mixed well (as shown by a magnified SEM image in Fig. 4). The elemental mapping indicates the formation of iron rich layer at the vortex since the distribution of iron is prominent in this vortex as well. Existing literature reports that while vortices are formed before and after the wave in a weld between metals of similar density, the weld shows single vortex before or after the wave for appreciably

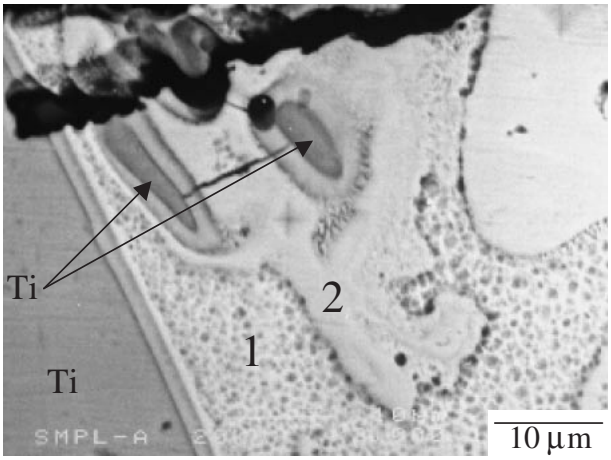

Fig. 4 SEM micrograph showing scan points of EDS analysis (E3).

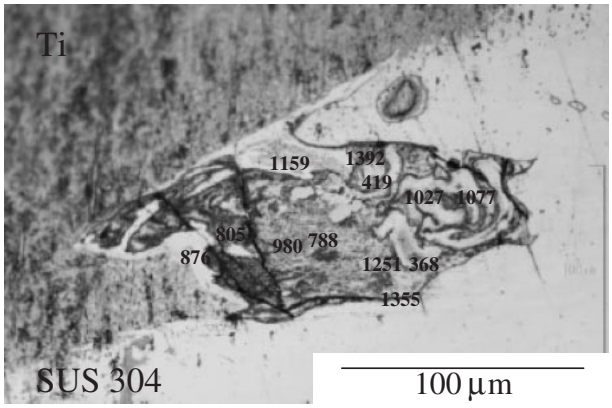

Fig. 5 Variation of microhardness values within the vortex (E7).

Table 2 Atomic percentage of the elements.

Point	Fe	Ti	Cr	Ni	Si
1	52	26	15	6	1
2	57	18	17.5	6.5	1

different densities.[4] Crossland *et al.*[24] concluded that the front vortices would mainly contain the parent plate material. This is in agreement with the atomic percentage of the elements, discussed in the next section. Microcracks can be seen (in Fig. 3) across the vortex. Residual stresses caused due to the difference in the heat transfer characteristics, brittleness of intermetallics, Shear stresses due to the difference in the elastic recovery of metals and the effects of rapid cooling contributes to cracking.

Figure 4 shows a SEM micrograph taken at the vortex with the scan points for EDS analysis. The atomic percentage of the elements is shown in Table 2. It can be observed that the fine-grained layer has a slightly different composition compared to the other point at the plane surface. The origin of these two layers may be attributed to the difference in the intense mixing of the participant metals within the vortex. It is noteworthy that the percentage of iron and titanium observed in the present study lies in the eutectic region of phase diagram for the formation of intermetallic compounds FeTi and Fe_2Ti. An unmixed part of titanium trapped in the vortex, shown by arrows, is also seen in Fig. 4.

The X-ray diffraction on the vortex was performed using Cu-Kα radiation for phase identification. The XRD results suggested the presence of both FeTi and Fe_2Ti intermetallic compounds dispersed in the vortex.

3.2 Micro hardness

The microhardness of titanium/stainless steel clad across the interface away from the vortices was measured at an interval of 1 mm using a load of 0.098 N. The results revealed an increase in hardness for both flyer and base plate close to the interface. The high hardness near the interface can be attributed to the intense plastic deformation during the collision of the plates. The hardness value remains constant at a distance of 2 mm away from the interface. These results were consistent with those reported by other researchers.[25,26] The results obtained from the vortices exhibited significantly different hardness values as shown in Fig. 5. The presence of stronger and stiffer FeTi and Fe_2Ti intermetallics led to an increase in the constraint to the localized plastic deformation of the material during the microhardness test. These values vary fairly across the vortex depending on the intermixing of the two components. In some part of the vortex, stainless steel remained unmixed shown by relatively low hardness in Fig. 5. It might be noted that no two vortices had the same values.

3.3 Microstructural variation

Figures 6(a) and (b) shows the microstructure of the interface for flyer thickness 5 mm. A sharp transition with a wavy topography between the participant metals can be observed. The pattern of these interfacial oscillations is sensitive to the parameters of the system. It can be seen that the amplitude and wavelength increased with the increase in the loading ratio (mass of explosive for unit mass of flyer plate) from 1.2 to 1.4. This is in agreement with the literature reports.[27–29] On the side of the wave crest a sizeable amount of jet is captured in the vortices, seen as dark regions along the wave. In comparison to the low loading ratio, the vortices on the high loading ratio are wider. Hokamoto *et al.*[17] reported that the amount of kinetic energy lost by the collision at the welded interface is a very important factor for the achievement of sound welding. The kinetic energy depends on the thickness of the flyer plate and the plate velocity in the system. In these experiments, the thickness of the plates were constant, hence the difference lies in the plate velocity, which increased the kinetic energy values. The magnified view of 'A' exhibiting thin interfacial layer at the bonding interface of the clad obtained under relatively high ΔKE condition is shown in Fig. 6(c). Nishida *et al.*[13] concluded that explosive welding is achieved by the melting of thin layers along the contact surface of both the materials.

Figure 7 shows the variation of the interfacial waves for 3 mm thick flyer explosive clads as a function of loading ratio and kinetic energy. The interface has a wavy microstructure that is consistent in general with those reported above. Amplitude and wavelength was observed to increase from the low loading ratio to the high loading ratio. It was observed

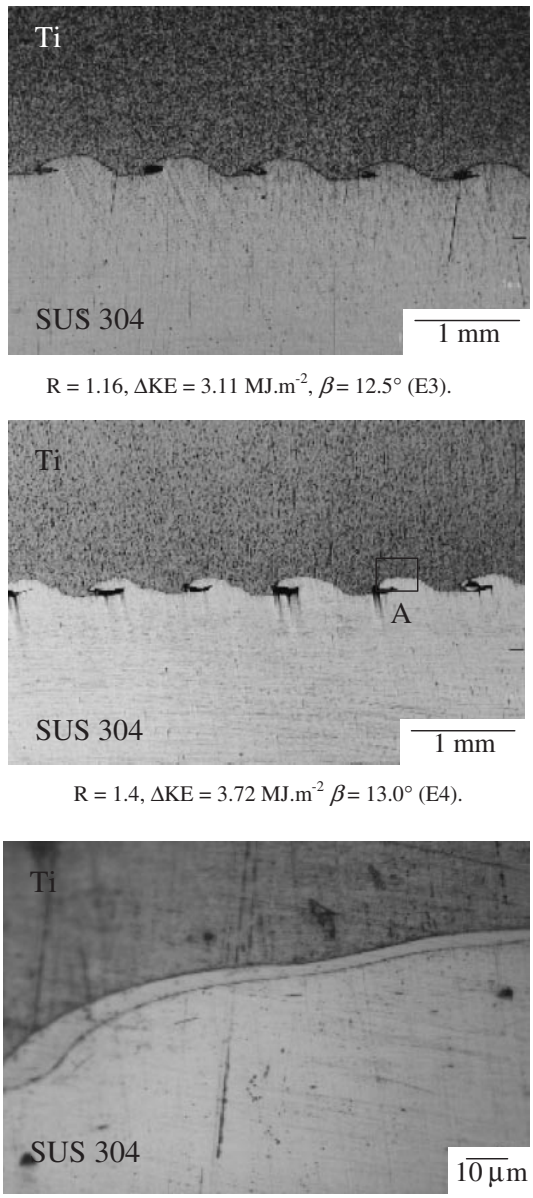

Fig. 6 (a) and (b) Optical micrographs showing variation of microstructure for flyer thickness 5 mm (c) Micrograph showing magnified view of A.

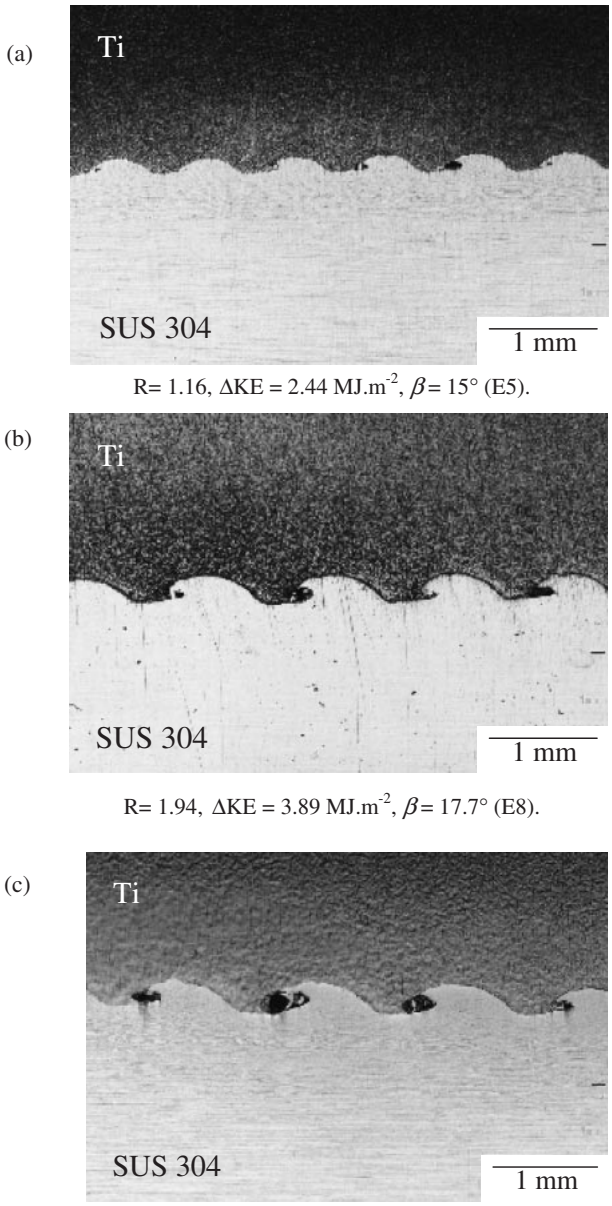

Fig. 7 Representative optical micrographs showing variation of microstructure for flyer thickness 3 mm.

that the average thickness of the vortices increased with the kinetic energy spent at the interface, as illustrated in Fig. 8. It is noted that an increase in the thickness of vortices has occurred at a kinetic energy of 2.44 MJ/m^2. At low kinetic energy loss the interfaces are smooth, and a further decrease in kinetic energy produces a flat interface.

It was noted that although the loading ratio is same (Figs. 6(a) and 7(a)), the kinetic energy spent at collision was different. One can note from the results that the dependence of loading ratio on the vortex formation becomes less obvious when the kinetic energy loss increases. In other words, the kinetic energy loss causes more shear deformation at the collision point. This argument is reasonable since the hump formed by the shear-deformed metal tends to trap the jet and form vortices. Therefore, kinetic energy loss at the interface plays a critical role in the microstructure of the clad. The focus was thus to establish the value of kinetic energy at which the formation of intermetallics could be fully avoided or reduced. The value of kinetic energy was found to be less when a thin flyer plate is used along the weldability region. The clad trials were then conducted with 1 mm flyer plate, as shown in Fig. 9. It was found that the interface shows a smooth wavy topography at a kinetic energy loss of 2.33 MJ/m^2, as shown in Fig. 9(a). When the kinetic energy was 2.08 MJ/m^2, the interface was observed to be flat, as shown in Fig. 9(b).

Nevertheless, the effect of loading ratio on the wavelength for different flyer thickness was observed. It was noted that although the loading ratio is same (Figs. 9(a), 7(c)) the wavelength is different. The micrographs displayed in Figs. 6, 7, 9 highlights the difference in the wavelength for different flyer thickness. This can be attributed to the variation in thickness of flyer plate that resulted in the change of wavelength due to the varied conditions at the

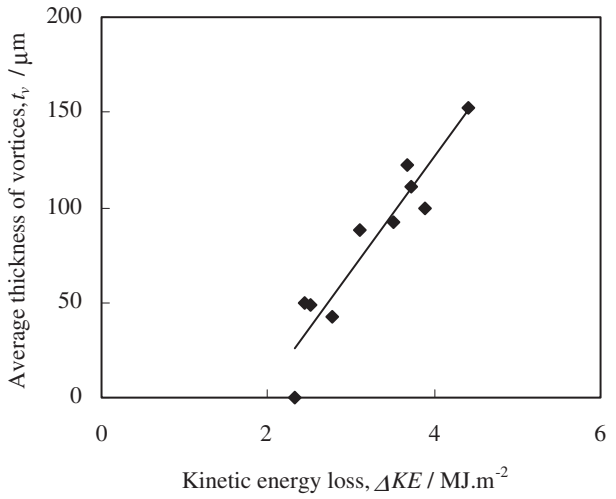

Fig. 8 Graphical representation showing the relation between kinetic energy loss and thickness of interfacial layer.

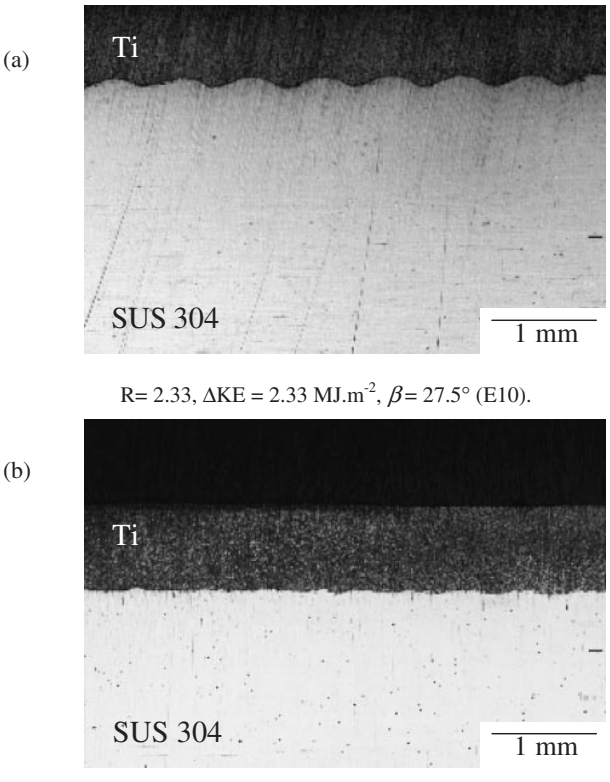

Fig. 9 Optical micrographs showing variation of microstructure for flyer thickness 1 mm.

collision point. The experimental results highlighted an independence of loading ratio for different flyer thickness and dependence for same flyer thickness. Deribas *et al.*[30] reported similar findings by varying the thickness of the base plate. The wavelength, λ, can be predicted by the following expression, for small angles of impact,[31]

$$\lambda \propto t_f \beta^2 \quad (4)$$

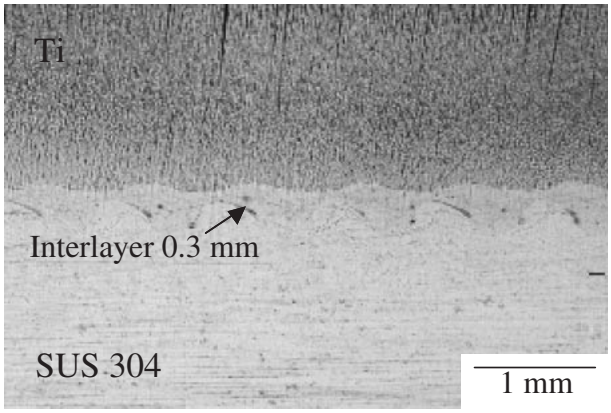

Fig. 10 Representative optical micrograph of multi layer welding using 304 stainless steel as an interlayer.

where t_f is the thickness of the flyer plate and β is the collision angle. This relationship agrees well with the experimental data for small angles of impact. There was a slight variation for angles exceeding 25°, in case of flyer thickness 1 mm. Based on the above expression, it can be deduced that if the thickness is small, the dynamic angle needs to be enhanced to attain same wavelength for different flyer thickness. Since the dynamic angle is influenced by the loading ratio, a high loading ratio is required for thin flyer plate as shown in Fig. 9. However, as the mass of the flyer plate is less, even at higher velocity the kinetic energy loss is minimized resulting in a wave devoid of intermetallics. We note with interest the shape of vortices formed in different flyer thickness. Although the vortices formed in same flyer thickness for different conditions are similar, there is a noticeable difference when the flyer thickness is varied. Instead of the wider and shorter vortices formed in thin flyer plate, the vortices formed in thick plates are stretched forward into the flyer plate. This would suggest that the vortex formation is controlled by the participant metal mass, thus explaining the differences in the vortices.

Obtaining a wavy interface from explosive welds seems to be straightforward, but that alone may not be sufficient for many applications if the bonding interface suffers from intermetallic problems. In the following, a strategy to achieve intermetallic free bonding interface is presented. It is certainly important to decrease the kinetic energy loss at the collision point so that vortices can be avoided. Hokamoto *et al.*[17] reported the use of a thin interlayer for the welding of aluminum/stainless steel. If a thick clad, and particularly thick titanium, is the goal, then the interlayer is needed to bring the kinetic energy under control to avoid the formation of vortices. Figure 10 shows a 3 mm thick titanium clad on to stainless steel using 0.3 mm interlayer of stainless steel at a loading ratio of 1.94. The stand off distance between titanium and interlayer was 10 mm and the interlayer and stainless steel base material was 5 mm. The kinetic energy dissipated at the collision was 0.54 MJ/m^2. The resulting intermetallic free bonding interface is attractive for pressure vessel fabrications.

Since the microstructure at the welded interface determines the mechanical properties, it is essential to evaluate the

bonding strength. Attempts to evaluate the tensile shear strength[4] of the samples were not satisfactory. While the sample with large waves (E3) exhibited 196 MPa, the strength of the sample with small waves (E6) was found to exhibit a significantly high value, 535 MPa. Both values are higher than the shear strength of titanium, but the values obtained here are uncertain due to inevitable interference of factors such as depth of milled slots and peeling action superimposed on the shear,[4] and the loading was done on a small area through one experiment for two different cases. In such cases, a dynamic test might well indicate the effect of unfavorable metallurgical condition over a large area. While in general the interfacial area increase with large waves, it is important to realize that in a dynamic test the strength can be reduced for following reason. The fracture toughness is considerably reduced at the vortex with cooling cavities and intermetallic compounds. This represents a potential source of weakness under impact conditions. This possibility is based on our experience through a series of experiments on repeated welding on the already bonded Ti/stainless steel plate, where the separation occurred along the interface of Ti/stainless steel for high kinetic energy conditions. We have therefore resorted to characterizing the micro structural variations to bring the kinetic energy under control, thus avoiding intermetallic phases. Detailed investigations related to multilayer welding using interlayer and dynamic response of three layer clads are the subjects of ongoing studies.

4. Conclusions

Explosive welding can be successfully used to clad commercially pure titanium and 304 stainless steel. The results of two layer welding, in general, revealed the characteristic wavy topography at the interface associated with the vortices. Kinetic energy loss was found to correlate well with the vortices featuring FeTi and Fe_2Ti intermetallics. An increase in the kinetic energy resulted in an increase in the vortices. The kinetic energy was found to be less for 1 mm flyer thickness compared to 3 and 5 mm flyer plates. The use of a thin flyer plate yielded the most satisfactory results in terms of interface devoid of intermetallics. Microhardness results showed an increase in the values at the interface and a gradual decrease away from the interface. Multi-layered welding using a thin stainless steel as an interlayer indicated a good interface as the kinetic energy dissipation at the collision was less.

Acknowledgements

This research is supported by the funding of 21st Century Center of Excellence program on Pulsed Power Science, Kumamoto University, Japan.

REFERENCES

1) J. Laermans and J. Banker: *Proc. of Corrosion Applications Conference*, (Wah Chang, 2003) pp. 157–165.
2) J. Banker: *Proc. of Reactive metals in Corrosive Applications Conference*, (Wah Chang, 1999) pp. 99–104.
3) A. Nobili, T. Masri and M. C. Lafont: *Proc. of Reactive Metals in Corrosive Applications Conference*, (Wah Chang, 1999) pp. 89–98.
4) B. Crossland: *Explosive welding of metals and its application*, (Oxford Univ. Press, Oxford, 1982).
5) A. S. Bahrani and B. Crossland: *Proc. Inst. Mech. Engr.* (1966) pp. 31–46.
6) A. A. Popoff: Mech. Eng. **5** (1978) 28–35.
7) C. R. Cowan, O. R. Bergmann and A. H. Holtzman: Met. Trans. **2** (1971) 3145–3155.
8) V. Shribman, A. S. Bahrani and B. Crossland: The Prod. Eng. (1969) 69–83.
9) K. Raghukandan: J. Mater. Process. Technol. **139** (2003) 573–577.
10) K. Hokamoto, A. Chiba, M. Fujita and T. Izuma: Comp. Eng. **5** (1995) 1069–1079.
11) K. Raghukandan, K. Hokamoto and P. Manikandan: Metals and Mat. Int. **10** (2004) 193–197.
12) Y. Morizono, M. Nishida and A. Chiba: Mater. Res. Soc. **458** (1997) 363–368.
13) M. Nishida, A. Chiba, Y. Honda, J. Hirazumi and K. Horikiri: ISIJ Int. **35** (1995) 217–219.
14) A. Nobili, J. G. Banker and C. E. Prothe: *Proc. of Reactive Metals Conference*, (Wah Chang, 2001) pp. 1–9.
15) P. Manikandan, K. Hokamoto, K. Raghukandan, A. Chiba and A. A. Deribas: Sci. Tech. Energetic Materials. **66** (2005) 370–374.
16) A. Deribas: *Impact Engineering and Application*, ed. by A. Chiba, S. Tanimura and K. Hokamoto, (Elsevier Science Ltd, UK, 2001) pp. 527–534.
17) K. Hokamoto, T. Izuma and M. Fujita: Metall. Trans. **24A** (1993) 2289–2297.
18) A. S. Bahrani, T. J. Black and B. Crossland: *Proc. Roy. Soc. Series A* **296** (1967) pp. 123–126.
19) G. R. Cowan and A. H. Holtzman: J. Appl. Phys. **34** (1963) 928–939.
20) O. R. Bergmann, G. R. Cowan and A. H. Holtzman: Trans. Met. Soc. of AIME. **236** (1966) 646–653.
21) T. Lyman: *ASM Metals Handbook: Metallography, Structures and Phase Diagrams*, **8** (Metals Park, Ohio, 1973).
22) W. Klein: *Doctoral Thesis of the Technical University*, (Clausthal, 1970).
23) J. D. Williams, P. Dhir and B. Crossland: *Proc. 3rd Int. Conf. of the Centre for High Energy Forming*, (1971) pp. 3.1.1–3.1.22.
24) B. Crossland and A. S. Bahrani: *Proc. 1st Int. Conf. of the Centre for High Energy Forming*, (1967) pp. 1.1.1–1.1.50.
25) U. Kamachi Mudali, B. M. Ananda Rao, K. Shanmugam, R. Natarajan and Baldev Raj: J. Nucl. Mater. **321** (2003) 40–48.
26) R. Kacar and M. Acarer: J. Mater. Process. Technol. **152** (2004) 91–96.
27) M. Acarer, B. Gulenc and F. Findik: J. Mater. Sci. **39** (2004) 6457–6466.
28) N. Kahraman and B. Gulenc: J. Mater. Process. Technol. **169** (2005) 67–71.
29) A. Durgutlu, B. Gulenc and F. Findik: Mater. Des. **26** (2005) 497–507.
30) A. A. Deribas, V. M. Kudinov, F. I. Matveenkov and V. A. Simonov: Fizika Goreniya i Vzryva **4** (1968) 100–107.
31) S. R. Reid: Int. J. Mech. Sci. **16** (1974) 399–413.